Video Article

Cerenkov Luminescence Imaging (CLI) for Cancer Therapy Monitoring

Yingding Xu[1], Hongguang Liu[1], Edwin Chang[1], Han Jiang[1], Zhen Cheng[1]

[1]Department of Radiology and Bio-X Program Canary Cancer at Stanford for Cancer Early Detection, Stanford University

Correspondence to: Zhen Cheng at zcheng@stanford.edu

URL: http://www.jove.com/video/4341
DOI: doi:10.3791/4341

Keywords: Cancer Biology, Issue 69, Medicine, Molecular Biology, Cerenkov Luminescence Imaging, CLI, cancer therapy monitoring, optical imaging, PET, radionuclides, Avastin, imaging

Date Published: 11/13/2012

Citation: Xu, Y., Liu, H., Chang, E., Jiang, H., Cheng, Z. Cerenkov Luminescence Imaging (CLI) for Cancer Therapy Monitoring. *J. Vis. Exp.* (69), e4341, doi:10.3791/4341 (2012).

Abstract

In molecular imaging, positron emission tomography (PET) and optical imaging (OI) are two of the most important and thus most widely used modalities[1-3]. PET is characterized by its excellent sensitivity and quantification ability while OI is notable for non-radiation, relative low cost, short scanning time, high throughput, and wide availability to basic researchers. However, both modalities have their shortcomings as well. PET suffers from poor spatial resolution and high cost, while OI is mostly limited to preclinical applications because of its limited tissue penetration along with prominent scattering optical signals through the thickness of living tissues.

Recently a bridge between PET and OI has emerged with the discovery of Cerenkov Luminescence Imaging (CLI)[4-6]. CLI is a new imaging modality that harnesses Cerenkov Radiation (CR) to image radionuclides with OI instruments. Russian Nobel laureate Alekseyevich Cerenkov and his colleagues originally discovered CR in 1934. It is a form of electromagnetic radiation emitted when a charged particle travels at a superluminal speed in a dielectric medium[7,8]. The charged particle, whether positron or electron, perturbs the electromagnetic field of the medium by displacing the electrons in its atoms. After passing of the disruption photons are emitted as the displaced electrons return to the ground state. For instance, one ^{18}F decay was estimated to produce an average of 3 photons in water[5].

Since its emergence, CLI has been investigated for its use in a variety of preclinical applications including *in vivo* tumor imaging, reporter gene imaging, radiotracer development, multimodality imaging, among others[4,5,9,10,11]. The most important reason why CLI has enjoyed much success so far is that this new technology takes advantage of the low cost and wide availability of OI to image radionuclides, which used to be imaged only by more expensive and less available nuclear imaging modalities such as PET.

Here, we present the method of using CLI to monitor cancer drug therapy. Our group has recently investigated this new application and validated its feasibility by a proof-of-concept study[12]. We demonstrated that CLI and PET exhibited excellent correlations across different tumor xenografts and imaging probes. This is consistent with the overarching principle of CR that CLI essentially visualizes the same radionuclides as PET. We selected Bevacizumab (Avastin; Genentech/Roche) as our therapeutic agent because it is a well-known angiogenesis inhibitor[13,14]. Maturation of this technology in the near future can be envisioned to have a significant impact on preclinical drug development, screening, as well as therapy monitoring of patients receiving treatments.

Video Link

The video component of this article can be found at http://www.jove.com/video/4341/

Protocol

1. Tumor Model

1. Culture H460 cells (American Type Culture Collection) in RPMI 1640 medium supplemented with 10% fetal bovine serum and 1% penicillin/streptomycin (Invitrogen Life Technologies). It should be noted that the choices of cell lines, culture mediums, locations of inoculation, number of xenografts per mouse, and other considerations are all to be tailored to the goals of a particular study. Here we will only present one specific project design to serve as an illustration.
2. Maintain cell lines in a humidified atmosphere of 5% CO_2 at 37 °C and change to fresh medium every other day.
3. When a 75% confluent monolayer of cells is formed, detach the monolayer with trypsin and dissociate cells into a single-cell suspension for further cell culture.
4. Suspend approximately 1 × 10^6 H460 cells in phosphate-buffered saline (PBS; Invitrogen) and implant subcutaneously in both left and right shoulders of nude mice (female athymic nude mice (*nu/nu*), 4 - 6 weeks old, Charles River Laboratories, Inc.).
5. Allow tumors to grow to 150 - 200 mm^3. It takes approximately 2 weeks for H460 tumor xenografts to grow to this size. Standard caliper measurement is carried out to track tumor sizes.
6. When tumors reach the ideal size the tumor bearing mice are now ready for treatment and *in vivo* imaging via both PET and CLI.

2. PET

1. Perform the PET studies according to this schedule or any variation of it depending on the specific project (**Figure 1**)[12]. A number of factors could influence the design of the schedule, including, but not limited to, choice of tumor xenograft cell lines, anticancer drugs, and dosing regimens. Here we will only present one specific imaging schedule. The CLI studies are to be performed according to the same schedule as those of the PET studies, with CLI performed immediately after the corresponding PET. It should be also noted here that the purpose of the PET studies is mainly for validation of the CLI results. For common users who just wish to use OI instruments for imaging radiolabeled probes, no PET is necessary. However, if one does desire PET validation it should be stressed that PET and CLI instruments must be located within very close proximity for the validation to be successful because of the short half life of ^{18}F (109.77 min).
2. Divide mice into treatment and control groups ($n \geq 3$ each). Treat mice in the treatment group with 2 injections of bevacizumab of 20 mg/kg at days 0 and 2. Day 0 is defined by the first injection. Note that at Day -1 a pre-scan should be performed via both PET and CLI.
3. Small-animal PET of tumor-bearing mice is to be performed with an R4 rodent model scanner (Siemens Medical Solutions USA, Inc.).
4. Anesthetize all mice with 2% isoflurane (Aerrane; Baxter) and inject with 3'-deoxy-3'-^{18}F-fluorothymidine (^{18}F-FLT; 7.3 - 8.0 MBq [198 - 215 µCi]) via the tail vein. The PET probe is to be diluted in PBS before injection.
5. After 1 hr, anesthetize mice again and place anesthetized mice prone and near the center of the field of view of the small-animal PET scanner.
6. Obtain three-minute static scans and reconstruct the images by a 2-dimensional ordered-subsets expectation maximum algorithm. Background correction is not necessary.
7. Draw regions of interest (ROIs; 5 pixels for coronal and transaxial slices) over the tumors on the decay-corrected whole-body coronal images. Obtain the maximum counts per pixel per minute from the ROIs and convert to counts per milliliter per minute by use of a calibration constant. With the assumption of a tissue density of 1 g/ml, convert the ROIs to counts per gram per minute. Determine image ROI-derived %ID/g values by dividing counts per gram per minute by injected dose. Attenuation correction is not necessary.

3. CLI

1. CLI is to be performed with an IVIS Spectrum system (Caliper Life Sciences). Acquisition and analysis of images are to be carried out using Living Image 3.0 software (Caliper Life Sciences). Wavelength-resolved spectral imaging is to be performed using an 18-set narrow-band emission filter (490 - 850 nm). Again, for each mouse, perform CLI immediately after PET to minimize the amount of radioactive decay if the PET studies are included in the protocol.
2. Place animals in a light-tight chamber under isoflurane anesthesia. Multiple mice can be placed simultaneously to increase throughput.
3. Acquire images using 3 min exposure time (f/stop=1, binning=4). Use the same illumination settings (lamp voltage, filters, f/stop, fields of view, binning) to acquire all images. Use the dorsal skin area to calculate the signal intensity of background tissue. Normalize fluorescence emission to photons per second per centimeter squared per steradian (p/s/cm^2/sr).

4. Representative Results

Visual comparison between CLI and PET images can be easily carried out. After unifying the scale bar across images from the same modality and place CLI and PET images side by side one can see in this representative panel (**Figure 2A**) that both CLI and PET revealed significantly decreased signals from H460 xenografts in treated mice from pre-treatment to day 3, suggesting significant therapeutic effect. As a comparison, moderately increased to unchanged signals were observed in untreated mice during the same time period (data not shown). By visual inspection alone one can observe that there is a good consistence between tumor contrasts that are visualized from CLI and PET. In fact, this visual correlation has sufficient resolution to show central necrosis of the tumor secondary to the anticancer treatment regimen (please compare the CLI and PET images from Day 3). To validate the imaging findings quantifications and correlation analysis can be carried out.

Quantifications of CLI and PET images and a simple fitting via linear regression showed that the two modalities indeed had an excellent correlation (**Figure 2B**, R^2=0.9309 for ^{18}F-FLT probed treatment group). Notably, in all of our CLI and PET imaging studies with different tumor models and different anticancer drugs the slopes of the fits are also remarkably close, thus suggesting an excellent fit of linear regression even of all data are conglomerated (data not shown). Both representative images are adapted from our previous publication[12].

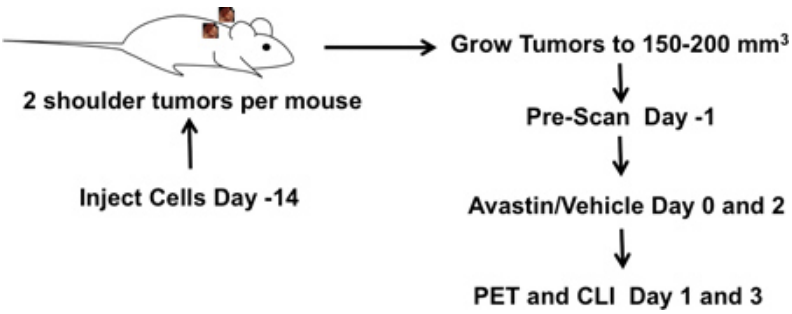

Figure 1. Schematic of experimental design of PET and CLI studies. Tumors were implanted bilaterally in shoulder region and allowed to grow to 150-200 mm^3, and tumor-bearing mice were subjected to *in vivo* imaging via PET and CLI at day -1, 1, and 3. Bevacizumab treatment was performed by 2 injections of 20 mg/kg at days 0 and 2.

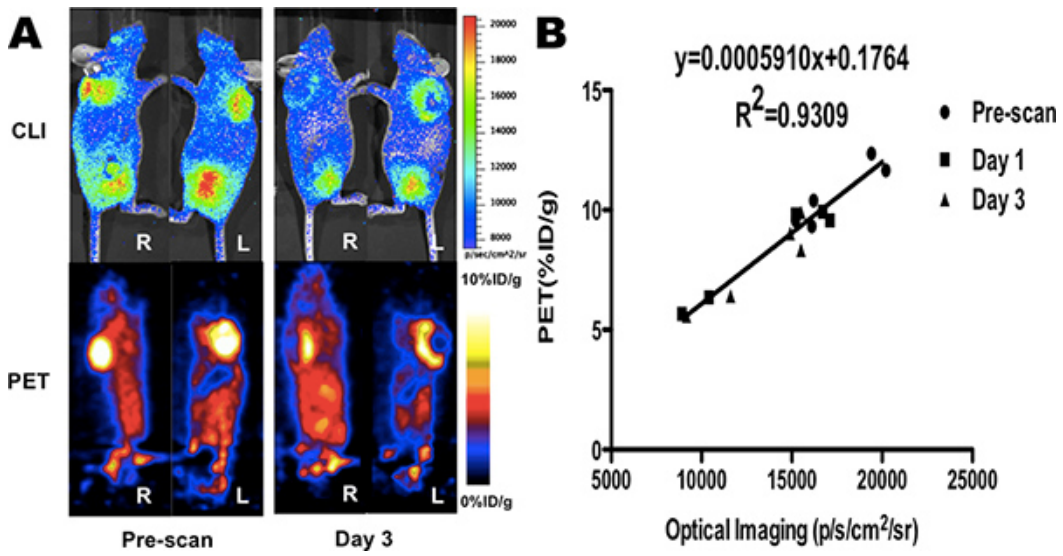

Figure 2. (A) *In vivo* CLI and PET images of mice bearing H460 xenografts treated with Bevacizumab before treatment (pre-scan) and after treatment (day 3). **(B)** Corresponding quantitative analysis of CLI and PET results (n=3) and their correlations. Images adapted from *(6)*. Click here to view larger figure.

Discussion

CLI is emerging as a promising molecular imaging technique that has found potentials in many basic science research applications and even clinical use[4,5,15,16,17]. The major advantages of CLI over traditional nuclear imaging modalities such as PET stem from its use of OI instruments, which are easier to use, characterized by short acquisition time and high throughput, significantly less expensive, and more widely available to researchers. Additionally, what sets CLI apart from OI in general is its use of β-emitting labeled molecules as imaging probes, many of which have been approved by the Food and Drug Administration (FDA), unlike traditional OI agents. With these unique and desirable qualities, CLI has quickly garnered attention from the field of molecular imaging. Yet its potentials in preclinical and clinical applications are yet to be fully investigated.

Cancer therapy monitoring is one of the areas where CLI can have some significant utility. It is a very important area that is key to probe development, drug screening, and even tailoring cancer therapy for patients. Currently, preclinical cancer therapy monitoring is carried out almost exclusively via nuclear imaging modalities such as PET. Therefore CLI provides a very attractive alternative to PET, particularly given that there is an excellent correlation between CLI and PET images. Yet, another advantage of CLI for therapy monitoring lies in the fact that CLI can image not only β^+-emitters, but also β^-emitters such as ^{32}P, ^{90}Y, and ^{131}I, all of which are clinically relevant.

However, CLI is not without flaws. The reliance on OI instruments dictates that CLI suffers from some shortcomings that are intrinsic to optical imaging such as signal attenuation and scattering in living tissues. Moreover, the particular spectrum of CR also results in limited signal intensity and subsequently, the deeper the signal from body surface, the lower the sensitivity, and the poorer the quantification capability[6]. However, while the shortcomings can be viewed to be significant, one can largely bypass these obstacles in preclinical research by employing small animals such as mice. More importantly, there are at least a couple of clinical areas that can potentially benefit from CLI cancer therapy monitoring. Monitoring superficial disease entities such as dermatological inflammatory conditions and cancers can serve as one good example. Moreover, disease entities that are deep yet accessible by charge-coupled device or fiber optic based techniques can use the excellent sensitivity and quantification capability of CLI as well. Yet another exciting possibility lies in using CLI to help surgeons obtain anatomic and functional information about tumors in the operating room. Two recent proof-of-concept studies have demonstrated detection and resection of tumors in mice with intraoperative image guidance thanks to CLI[18,19].

Disclosures

No conflicts of interest declared.

Acknowledgements

We acknowledge support from the National Cancer Institute (NCI) R01 CA128908 and Stanford Medical Scholar Research Fellowship. No other potential conflict of interest relevant to this article was reported.

References

1. Weissleder, R. & Mahmood, U. Molecular imaging. *Radiology.* **219** (2), 316 (2001).

2. Chen, K. & Chen, X. Positron emission tomography imaging of cancer biology: current status and future prospects. *Semin. Oncol.* **38** (1), 70 (2011).
3. Solomon, M., Liu, Y., Berezin, M.Y., *et al.* Optical imaging in cancer research: basic principles, tumor detection, and therapeutic monitoring. *Med. Princ. Pract.* **20** (5), 397 (2011).
4. Liu, H., Ren, G., Miao, Z., *et al.* Molecular Optical Imaging with Radioactive Probes. *PLoS One.* **5** (3), e9470 (2010).
5. Robertson, R., Germanos, M.S., Li, C., *et al.* Optical imaging of Cerenkov light generation from positron-emitting radiotracers. *Phys. Med. Biol.* **54** (16), N355 (2009).
6. Xu, Y., Liu, H., & Cheng, Z. Harnessing the power of radionuclides for optical imaging: Cerenkov luminescence imaging. *J. Nucl. Med.* **52** (12), 2009 (2011).
7. Cerenkov, P. Visible emission of clean liquids by action of g-radiation. *Dokl Akad Nauk SSSR 2.* **2**, 451 (1934).
8. Cerenkov, P. A. Visible radiation produced by electrons moving in a medium with velocities exceeding that of light. *Phys Rev.* **52** (4), 0378 (1937).
9. Boschi, F., Calderan, L., D'Ambrosio, D., *et al.* In vivo ^{18}F-FDG tumour uptake measurements in small animals using Cerenkov radiation. *Eur. J. Nucl. Med. Mol. Imaging.* **38** (1), 120 (2011).
10. Liu, H., Ren, G., Liu, S., *et al.* Optical imaging of reporter gene expression using a positron-emission-tomography probe. *J. Biomed. Opt.* **15** (6), 060505 (2010).
11. Park, J.C., Yu, M.K., An, G.I., *et al.* Facile preparation of a hybrid nanoprobe for triple-modality optical/PET/MR imaging. *Small.* **6** (24), 2863 (2010).
12. Xu, Y., Chang, E., Liu, H., *et al.* Proof-of-concept study of monitoring cancer drug therapy with cerenkov luminescence imaging. *J. Nucl. Med.* **53** (2), 312 (2012).
13. L.M., Ellis Bevacizumab. *Nat. Rev. Drug Discov.*, Suppl. S8 (2005).
14. Hochster, H.S. Bevacizumab in combination with chemotherapy: first-line treatment of patients with metastatic colorectal cancer. *Semin. Oncol.* **33** (5 Suppl. 10), S8 (2006).
15. Dothager, R.S., Goiffon, R.J., Jackson, E., *et al.* Cerenkov radiation energy transfer (CRET) imaging: a novel method for optical imaging of PET isotopes in biological systems. *PLoS One.* **5** (10), e13300 (2010).
16. Hu, Z., Liang, J., Yang, W., *et al.* Experimental Cerenkov luminescence tomography of the mouse model with SPECT imaging validation. *Opt. Express.* **18** (24), 24441 (2010).
17. Park, J.C., Il An, G., Park, S.I., *et al.* Luminescence imaging using radionuclides: a potential application in molecular imaging. *Nucl. Med. Biol.* **38** (3), 321 (2011).
18. Holland, J.P., Normand, G., Ruggiero, A., *et al.* Intraoperative imaging of positron emission tomographic radiotracers using Cerenkov luminescence emissions. *Mol. Imaging.* **10** (3), 177 (2011).
19. Liu, H., Carpenter, C.M., Jiang, H., *et al. J. Nucl. Med.* Submitted, (2012).

